Assessment of Damage of Glutathione by Glow Discharge Plasma at the Gas–Solution Interface through Raman Spectroscopy[a]

Zhigang Ke, Zengliang Yu, Qing Huang*

Although non-thermal discharge plasma is more and more applied in biological field, the molecular mechanisms of plasma acting on biomolecules are still unclear, which are indispensable for understanding the plasma-induced biological effects. In this work, discharge plasma at the gas–solution interface was employed to irradiate on reduced glutathione (GSH), the most abundant low molecular weight thiol-containing antioxidant in cells. Through Raman spectroscopy, both the irreversible damage and reversible conversion of GSH to oxidized glutathione (GSSG) were monitored in a non-destructive fashion, so that the reaction kinetic processes through multi-pathways could be evaluated quickly and quantitatively. Based on the experimental data, the reaction mechanism was discussed.

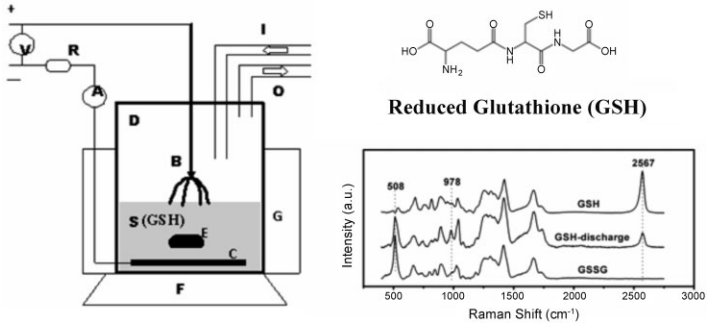

1. Introduction

Since non-thermal discharge plasma formed in contact with liquid water can be employed to irradiate on various types of materials such as biological substances, it has been widely applied for many practical usages, including chemical analysis,[1] material processing,[2–4] pollution control,[5–11] and inactivation of cells and microbes.[8,12–16] As a form of advanced oxidation–reduction processes (AORP), discharge plasma can induce the generation of large number of oxidative and reductive free radicals, such as hydroxyl radical, hydrogen radical, aqueous electron, and so on.[17–19] Most applications of this technique are dependent on the reactions of the dissolved materials/pollutants with the generated chemical reactive species. For example, as for the environmental application, the generated reactive species can be used directly to degrade or remove pollutants from solution,[5–8] or to modify the physicochemical properties of absorbents.[9–11]

As no costly equipment is required plasma sterilization is easily adaptable to complex devices and conventional processes, such as surgical instruments. The sterilization process is usually conducted at room temperature and does not involve any chemicals, and hence, it poses no dangers associated with high temperature and is non-toxic. Furthermore, plasma treatment for sterilization is fast, usually in the order of minutes or less.[20] Therefore, it is fast evolving into a promising alternative to standard sterilizing techniques. Indeed, it is necessary not only to study the lethal effect of plasma on microbes at the

Z. Ke, Z. Yu, Q. Huang
Key Laboratory of Ion Beam Bio-engineering, Institute of Technical Biology and Agriculture Engineering, Hefei Institutes of Physical Science, Chinese Academy of Sciences, Hefei 230031, China
E-mail: huangq@ipp.ac.cn
Q. Huang
University of Science and Technology of China, Hefei 230026, China

[a] **Supporting Information** is available from the Wiley Online Library or from the author.

DOI: 10.1002/ppap.201200047

cellular level, but also to explore the effect and mechanism of plasma at the biomolecular level because the latter is indispensable for understanding the chemical reactions and changes of biomolecules occurred within cells during plasma treatment. Up to now, there are some published papers with the plasma-induced effects on biomolecules.[21–28] For example, Yan et al. have indicated that plasma plume could cause plasmid DNA topological alteration, as manifested by the transformation of supercoiled form to open circular and linearized form detected by agrose gel electrophoresis.[21] It is the reactive species formed during plasma treatment, instead of heat, ultraviolet radiation, and intense electric field, that break the double strand of plasmid DNA.[22] The effect of plasma on some model proteins has also been investigated by some researchers. Kong's group have evidenced that glow discharge can induce the destruction and degradation of proteins deposited on stainless-steel surfaces, implying that this technique can be used as an effective sterilization technology for surgical instruments contaminated by proteinaceous matters.[23,24] In addition, protein dissolved in solution can also be easily inactivated and degraded by discharge plasma formed in contact with liquid water.[25,26,28] Although so many studies have been reported on the effect of plasma on the activity and conformation of biomacromolecules, but the corresponding molecular mechanisms are still elusive. This situation is partially owing to the reason that there is a lack of effective tool which can assess the involved chemical reactions quickly, quantitatively, and non-invasively.

Previously, our group have reported the damage of amino acids (phenylalanine and cysteine) and bases by non-thermal discharge plasma at the gas–solution interface.[29–31] In this paper, the damage of reduced glutathione (γ-L-glutamyl-L-cysteinyl-glycine, GSH) under the same conditions was investigated. GSH is considered as the most abundant low molecular weight thiol-containing antioxidant in vivo,[32] with concentration in the range of 1–10 mM in the cytosol of cells.[33] The mechanism of protection against oxidative stress by GSH involves two reaction pathways. One is the scavenging of damaging free radicals, such as hydroxyl radical, and the other is the transfer of hydrogen from GSH to damaged target molecules.[34] In both pathways, thiyl radical ($GS^{\bullet}$) is the most prominent sulfur intermediate, and two thiyl radicals can dimerize to form one oxidized glutathione (GSSG). [GSH]/[GSSG] ratio, which is larger than 10 under normal physiological conditions, is a sensitive indicator of oxidative stress of cells.[35] Both GSH concentration and [GSH]/[GSSG] ratio have usually been utilized as a reflection of oxidative stress under various conditions. Most of the methods for quantifying GSH concentration are based on the derivation of the sulfhydryl group with absorbance or fluorescence probes.[36]

In the current work, the change of the state of sulfur in GSH and the GSH–GSSG conversion under argon discharge plasma were quantitatively investigated by using Raman spectroscopy, which has been proved to be very useful for protein/peptide analysis.[37–44] Also, the kinetics of GSH degradation and GSSG formation were scrutinized, in the hope that it may provide us a better understanding of the mechanism of discharge plasma acting on sulfhydryl in proteins.

2. Experimental Section

2.1. Chemicals

All the chemicals used in our experiments were obtained from Sangon Biotech (Shanghai) Co., Ltd. as the analytical grade and used without further purification. All the aqueous solutions were made using distilled water.

2.2. Discharge Apparatus

The construction of the experimental set-up has been reported previously.[29] Briefly, a needle-like anode and a plate-like cathode, both of which are made of stainless steel, were placed ≈3–5 mm above the solution surface and submerged in the solution, respectively. Both electrodes were connected to a DC power supply. After discharge spark ignition the voltage was lowered to about 1 300 V (±10%, $I = 40$ mA, reactor power (P) = 52 W) and stabilized during the discharge. Argon was preferred as the discharge atmosphere due to its non-reactive nature and introduced into the reactor before discharge in order to remove air. Certain volume of samples was drawn from the reactor periodically and analyzed immediately.

2.3. Sample Analysis

2.3.1. Evaluation of GSH Damage and GSH–GSSG Conversion through Raman Spectroscopy

Raman spectra were acquired with a HORIBA JOBIN YVON XploRA spectrometer equipped with a 532 nm solid laser, 9.0 mW. The spectrometer worked in the confocal mode, where a 100× objective (Olympus, MPlanN, NA 0.9) was used to focus the laser onto the sample (with spot size ≈3 μm in diameter) and also collect the back-scattered Raman light into the detector. Under our experimental conditions, the laser power at the sample was reduced to approximately 5.0 mW. For Raman measurement, a volume of 10 μL sample solution was deposited onto quartz substrate and allowed to dry at 60 °C for 5 min and spectra were collected on the edge of the "coffee-ring" formed on the edge of drop arising from the outward flow of solvent,[45] as shown in Supporting Information Figure S1. All the spectra shown in this work represent the average from four cycles of 30 s Raman spectra acquired consecutively under the same conditions. Spectra analysis was performed with the NGSLabSpec software (HORIBA JOBIN YVON).

DOI: 10.1002/ppap.201200047

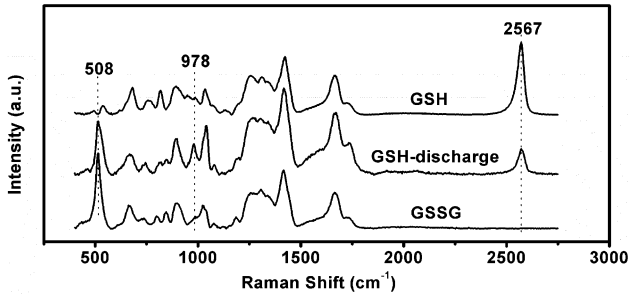

Figure 1. Raman spectra of GSSG and GSH before and after discharge for 6 min.

2.3.2. Determination of Hydrogen Sulfide

Production of hydrogen sulfide from GSH solution during discharge was measured colorimetrically by means of the molybdate reagent[46] and the details can be found in our previous studies and the references cited therein.[30]

3. Results and Discussion

3.1. Validation of the Quantification of [GSH] and [GSSG]/[GSH] Ratio through Raman Spectroscopy

Drops (10 μL) of freshly prepared mixture of GSH and GSSG with GSH concentration in the range 1–10 mM were deposited onto quartz substrates for drying at 60 °C for 5 min and the "coffee-ring" drying patterns were formed as expected. A quartz substrate was chosen because it exhibits minimal interference with the Raman spectra of GSH and GSSG. Raman spectra of the samples were systematically collected by focusing the laser on the surface of the "coffee-ring" pattern. In Figure 1, the reference Raman spectra of GSH and GSSG are shown in the range 400–2 750 cm^{-1}. Obviously, the Raman band of the −SH stretching vibration at 2 567 cm^{-1} [47] and the −S−S− stretching vibration at 508 cm^{-1} [48] are the characteristic band of GSH and GSSG, respectively. The fact that minimal Raman signal from both the quartz substrate and GSSG overlap with the band of −SH stretching vibration makes it possible to utilize the Raman intensity at 2 567 cm^{-1} as the reference for GSH quantification. As shown in the inset of Figure 2a the intensity of Raman signal at 252 cm^{-1} remained largely unchanged for the mixture with different GSH concentration. Similar results were obtained with GSH solution before and after discharge treatment (see the inset of Figure 3a below). Therefore, all the Raman spectra were normalized with the signal at 252 cm^{-1} and then the peak heights at 2 567 cm^{-1} were utilized to create standard curve for GSH quantification. The result is illustrated in Figure 2a, showing clearly the validity of the Raman spectral analysis for accurately quantifying GSH in the GSH–GSSG mixture. Moreover, since the ready conversion of the sulfhydryl to disulfide and the biological importance of GSH–GSSG system in organisms, it is of great significance to accurately and rapidly determine the [GSSG]/[GSH] ratio for estimating the oxidative stress under various conditions. Therefore, the [GSSG]/[GSH] ratio was also quantitatively investigated by analyzing the spectra of the mixture (another set of mixture of GSH and GSSG) after subtracting the background signal of quartz substrate. The ratio of the intensity of −S−S− stretching vibration at 508 cm^{-1} to the intensity of −SH stretching vibration at 2 567 cm^{-1} was used as the reference and a standard curve was made for quantifying [GSSG]/[GSH]. Also, a linear relationship was obtained between [GSSG]/[GSH] and I508/I2567, as shown in Figure 2b.

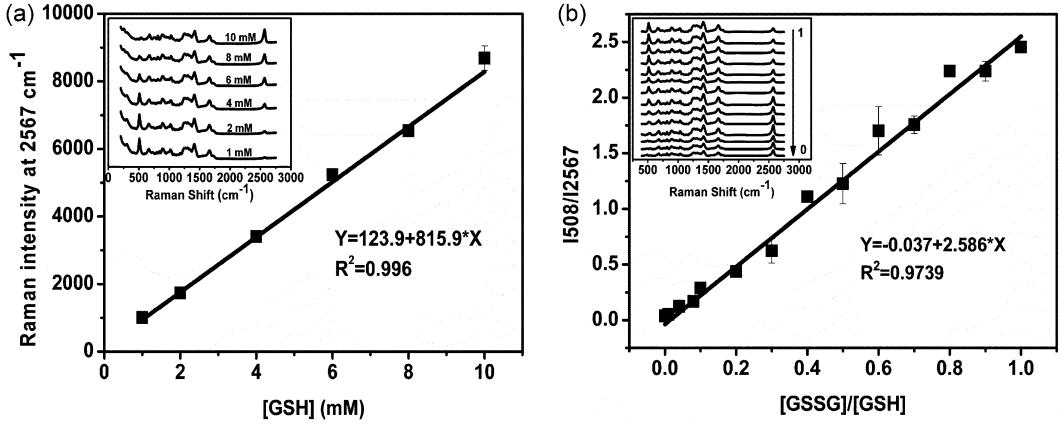

Figure 2. Standard curve for determining (a) GSH and (b) [GSSG]/[GSH] ratio via Raman method; Inset: (a) Raman spectra of the mixture of GSH and GSSG with different GSH concentration; [GSSG]: 0–4.5 mM; (b) Raman spectra of the mixture of GSH and GSSG with different [GSSG]/[GSH] ratios. The arrow in the inset means the change of [GSSG]/[GSH] ratio. [GSH]: 2.5–5 mM, [GSSG]: 0.2–2.5 mM. All the data points present the average of two measurements.

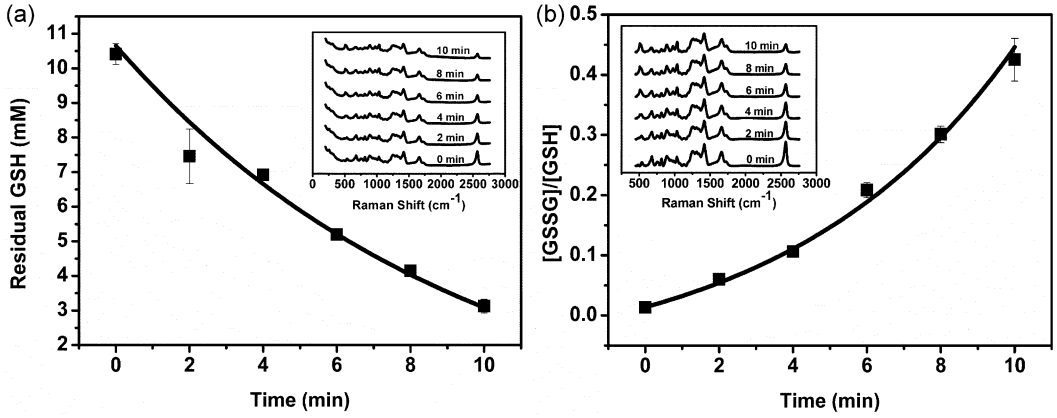

Figure 3. (a) The residual GSH content and (b) [GSSG]/[GSH] ratio as a function of discharge time detected by Raman spectroscopy; Inset (a) and (b): Raman spectra of GSH after discharge treatment for different periods of time with different spectra analysis. All the data points present the average of two measurements.

3.2. Damage of GSH by Argon Discharge Plasma

Based on the successful quantification of GSH via Raman spectroscopy, the damage of GSH induced by argon discharge plasma taking place at the gas–solution interface was quantitatively estimated. Raman spectra of GSH solution with original concentration at 10 mM after plasma treatment for different periods of time were collected and normalized at 252 cm^{-1} as detailed above. The residual GSH contents were calculated according to the standard curve in Figure 2a and the result is illustrated in Figure 3a. The primary GSH concentration calculated according to the standard curve before discharge is 10.4 mM, which is in accordance with the actual content (10 mM). The GSH damage follows the exponential law and its concentration falls from 10.4 to 3.1 mM with the discharge time for 10 min. The influence of the change of solution pH induced by discharge on GSH Raman spectra can be ruled out via control experiments. The solution pH decreased from 3.1 to 2.7 after argon discharge treatment for 10 min. No change of both the −SH stretching vibration frequency and intensity in Raman spectra for GSH solution with original pH 3.1 or 2.7 was observed (Figure S2 in Supporting Information), indicating that the change in Figure 3a was solely due to the reactions induced by discharge but not the solution's pH change. The data in Figure 3a are fitted as follows:

$$\ln\left(\frac{C_0}{C_t}\right) = kt$$

where C_0 and C_t represent the concentration of GSH before and after discharge treatment for t minutes, respectively, and k is the rate constant. The k value is 0.11 min^{-1} for the degradation of GSH induced by discharge plasma in argon atmosphere.

3.3. Formation of GSSG and Quantification of [GSSG]/[GSH]

As illustrated in radiation chemistry, sulfhydryl group is the major target attacked by the produced reactive species during irradiation on sulfhydryl-containing amino acids, peptides, and proteins.[49] Several products are formed from radiolysis of sulfhydryl-containing chemicals, and usually, formation of disulfide bond is one of the main results.[50] Many factors including oxygen concentration, pH, and so on can affect the yield of different products. For example, G(-RSH), G(RSSR), and G(H_2S) (yields per 100 eV) are 36.3, 15.5, and 2.35, respectively, for γ-radiolysis of 3.0×10^{-3} M cysteine solution in the presence of 9.75×10^{-5} M oxygen at pH 7.0; whereas they changed to 37.1, 17.7, and 2.0, respectively, when the oxygen concentration increased to 2.2×10^{-4} M.[50] In another report, it was detected that almost all damaged cysteine by γ-irradiation were converted to cystine at pH 3.0 in the presence of oxygen.[49] Similarly, the sulfhydryl group in cysteine is also susceptible to the reactive species produced by discharge plasma, as previously reported by us.[30] In the present work, Raman spectroscopy was used to investigate the change of the state of sulfur of GSH as a result of discharge plasma treatment. As seen from Figure 1, the most striking differences of GSH Raman spectra before and after discharge are both in the −SH and −S−S− stretching vibration region: the Raman peak of −S−S− stretching vibration at 508 cm^{-1} appeared after discharge treatment, concomitantly with a decrease in the intensity of the −SH stretching vibration band at 2 567 cm^{-1}. The decrease in the intensity of the 2 567 cm^{-1} band along with the increase in the intensity of the 508 cm^{-1} band unambiguously confirms that the sulfhydryl group in GSH were converted to disulfide. The accurate [GSSG]/[GSH] ratio of GSH solution with different periods of discharge

DOI: 10.1002/ppap.201200047

time were calculated according to the standard curve in Figure 2b and the result is shown in Figure 3b. The molar ratio increases exponentially from 0 to 0.43 as the discharge time from 0 to 10 min.

A comprehensive analysis of the data in Figure 3a and b reveals the actual GSSG concentration and the percentage of GSH converted to GSSG in the reduced GSH. The results are illustrated in Figure 4, where the proportion of GSH converted to GSSG to the reduced GSH is about 30–40%, which means that about 70–60% reduced GSH were converted to other products. It thus suggests other products must have been produced during the discharge, such as formation of hydrogen sulfide (discussed below). Actually, as shown in Figure 1, a new Raman band at 978 cm^{-1} emerged after discharge treatment, which belongs to neither GSH nor GSSG. This just gives another solid evidence for the formation of other product except GSSG.

For comparison, the fluorescence spectroscopy method[51] introduced by Senft et al. was also applied for determining GSH and GSSG in GSH solution after argon discharge treatment (see Figure S3 in Supporting Information). The proportion of the GSH converted to GSSG to the reduced GSH detected by this method is about 40–70%, much higher than the data determined by Raman spectroscopy. The reason for this difference is that high concentration of hydrogen peroxide was formed in solution by discharge treatment[6] and more GSSG was formed due to the action of produced hydrogen peroxide on GSH during storage of the treated sample. Because the fluorescence method is much more time-consuming and the determination cannot be accomplished immediately after discharge treatment, therefore, here it shows that in this case the Raman spectroscopy method is indeed a more effective way which can provide a more accurate evaluation.

3.4. Relative Damage of the Main Chain to the Side Chain in GSH

The foregoing section has discussed the susceptibility of the side chain of amino acid and thiol-containing peptide to discharge plasma. Moreover, the main chain of peptide and protein can also be damaged by the produced reactive species. Quantitative or semiquantative determination of the damage of the main chain relative to the side chain in peptide and protein is crucial for illustrating the mechanism of plasma-induced modification of the structure and function properties for the important biomolecules. Herein, the damage of the peptide bond of GSH relative to the sulfhydryl group was determined as a function of discharge time by Raman spectroscopy. As reported previously, the Raman band located at 1 662 cm^{-1} is due to the amide I vibration.[52] Therefore, the ratio I1662/I2567 was employed to probe the damage of peptide bond relative to sulfhydryl group of GSH under discharge plasma, and the result is depicted in Figure 5. It shows that the I1662/I2567 ratio exponentially increased from 0.58 to 1.59 as the discharge time from 0 to 10 min, suggesting that the sulfhydryl group is more susceptible to the attack by the produced reactive species during discharge.

3.5. Formation of Hydrogen Sulfide

Except for the reversible damage of sulfhydryl group of GSH to disulfide, irreversible damage for production

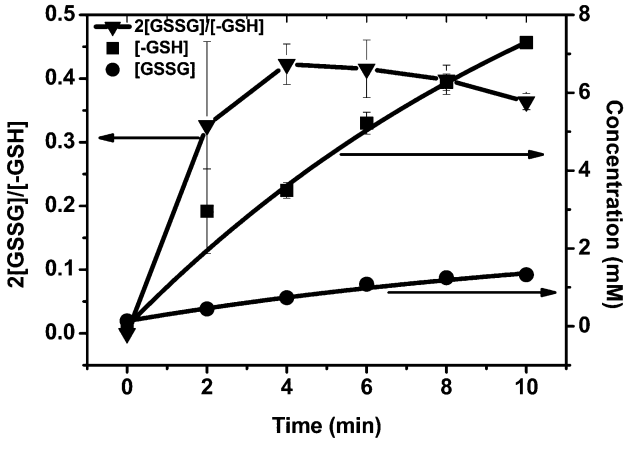

Figure 4. The reduced GSH and produced GSSG concentration and the percentage of GSH converted to GSSG. All the data points present the average of two measurements.

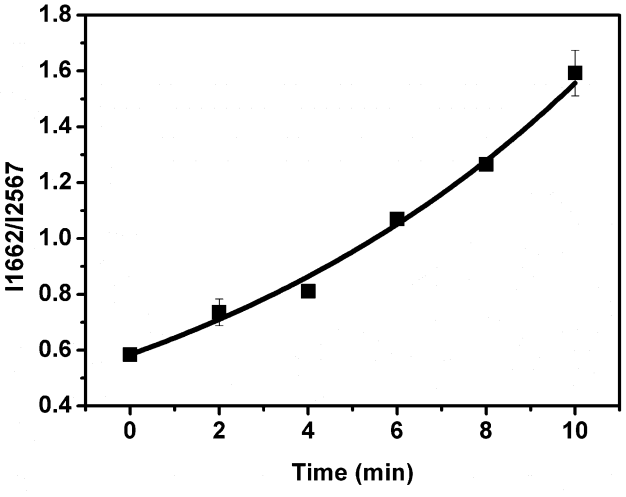

Figure 5. The ratio of the Raman intensity of the amide I vibration (1 662 cm^{-1}) to the intensity of –SH stretching vibration (2 567 cm^{-1}) as a function of discharge time. All the data points present the average of two measurements.

of hydrogen sulfide was also observed by applying molybdate reagent to the discharge-treated system, similar to the case of cysteine as we reported previously.[30] It is also of great importance from the biological point of view since its production within cells is likely toxic. After collecting the gas emitted from the gas outlet, the reagent presented amethyst with maximum absorption at 670 nm, while the control showed no color change and no absorption in the same region. A positive correlation between the content of produced hydrogen sulfide and discharge time was observed, as shown in Figure 6.

3.6. Mechanisms

When high voltage is applied to generate discharge plasma at the gas–solution interface, energetic ions, mainly being H_2O^+ and including gas ions with one positive charge, are produced in the cathode dark space by the electron impact ionization of water vapor and gas molecules in the gas phase. Water molecules in solution are ionized and activated by collision with these positive ions under the acceleration of cathode drop near the solution surface, followed by formation of primary free radicals, including hydroxyl radical, aqueous electron, hydrogen radical, and so on.[5,17–19]

$$e + H_2O \rightarrow H_2O^+ + 2\,e_{aq}^-$$

$$e + Ar \rightarrow Ar^+ + Ar^* \ldots$$

$$H_2O + H_2O^+/Ar^+(Ar^*) \rightarrow HO^\bullet + e_{aq}^- + H^\bullet \ldots$$

GSH is then damaged upon the attack by these primary free radicals and thiyl radicals are produced. GSSG are formed via dimerization of produced thiyl radicals or reaction between thiyl radicals and GSH (GS^-) (reaction 1–8), as elucidated by the radiation chemistry.[53,54]

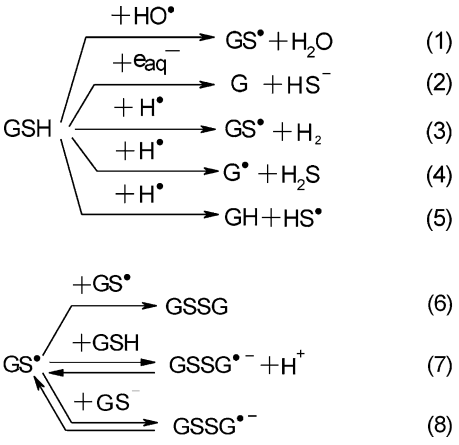

When $\ln(C_t/C_0)$ was plotted versus time, a good linear correlation was obtained, which indicated that GSH damage by discharge plasma fitted first order kinetics. The results implied that GSH was mainly damaged directly by the plasma-generated reactive species via reactions (1)–(5). The pK_a value of the sulfhydryl in GSH is 9.12,[55] which means most sulfhydryl is in protonated form and reaction (8) is neglectable in our experimental conditions (pH 3.1). GSH can scavenge all the water primary radicals, and therefore reactions (1)–(5) may exist during plasma treatment. As shown in Figure 4 that about 30–40% damaged GSH were converted to GSSG detected by Raman spectroscopy, it is reasonable to estimate that >30–40% damaged GSH were converted to $GS^\bullet$ (reaction (1) and (3)) assuming that GSSG were mainly formed via reaction (6). GSSG is also susceptible to chemical reactive species, and therefore it was also being damaged during plasma treatment. This can be confirmed by the data shown in Figure S3 where detected GSSG concentration increased linearly from 0 to 6 min and then decreased. It means that when the formed GSSG accumulated a certain concentration, the appearance of destruction of GSSG by plasma treatment became dominant. In addition, produced $GS^\bullet$ can also decay via other reaction pathways besides reaction (6). For example, thiyl radicals can decay via intramolecular rearrangement reaction by which the hydrogen of CH_2 group at the α-position transfers to sulfur atom leading to the formation of carbon-centered radicals.[56,57] So, we speculate that more than 30–40% damaged GSH molecules were attacked by hydroxyl radical and hydrogen atom via reaction (1) and (3) to form $GS^\bullet$, which were further dimerized to form GSSG.

A large number of published literatures have confirmed that hydroxyl radical is a prominent reactive species accounting for the observed plasma-induced phenomenon due to its strong oxidation capability.[58,59] It has been evidenced that hydroxyl radical and hydrogen peroxide

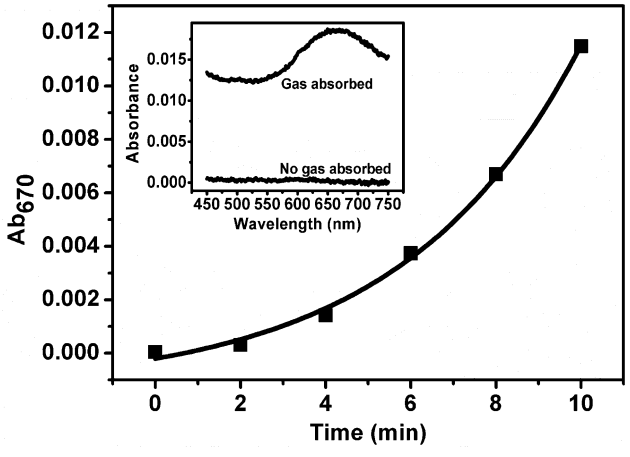

Figure 6. Detecting and quantifying the produced hydrogen sulfide.

DOI: 10.1002/ppap.201200047

were primarily responsible for plasma-induced angiogenesis.[58] Indeed, we have detected that H_2O_2 concentration in solution generated by plasma treatment in our experimental conditions was as high as millimolar level,[6] implying that large number of hydroxyl radicals were generated since H_2O_2 can be considered as a useful, although not perfect, indicator species for hydroxyl radicals in plasma system.[60] Therefore, hydroxyl radicals must play an important role in GSH damage and $GS^{\bullet}$ formation.

Except for hydroxyl radical the hydrogen radical should also contribute to $GS^{\bullet}$ formation. It not only originated from the dissociation of water molecules, but also from the neutralization of aqueous electron by hydrogen ion in acid solution as in our experimental conditions (pH 3.1).[18,61] Littman et al. have examined the products of aqueous phase reactions between hydrogen radical and cysteine and found that the cystine was the main product in acid or neutral solution.[62] The formation mechanism was explained satisfactorily by reaction (3). Markakis and Tappel[63] have also suggested that reaction (3) was the major primary reaction between hydrogen radical and cysteine. Possessing the similar structure feature with cysteine, GSH reacts with the radicals in the similar way as cysteine. However, respective contribution of hydroxyl radical (reaction 1) and hydrogen radical (reaction 3) to $GS^{\bullet}$ formation cannot be distinguished from our data.

As described in reaction (2), (4), and (5), hydrogen sulfide can be produced from the reactions between GSH and aqueous electron or hydrogen radical. In our experimental conditions reaction (2) can be excluded because almost all the aqueous electrons were scavenged as mentioned above, and therefore, hydrogen radical was the main contributory factor for hydrogen sulfide formation. Markakis and Tappel.[63] have measured the product yields of γ-irradiation of aqueous solutions of cysteine and cystine under various conditions and suggested that both reaction (4) and (5) occurred to some extent but that reaction (4) was much faster than (5). From the rate of hydrogen sulfide formation Navon and Stein[64] have estimated that about one-fifth of reacted cysteine with hydrogen radical yielded hydrogen sulfide.

The effect of UV irradiation generated during discharge plasma on GSH damage was also studied. Certain volume of GSH solution (10 mM) were enclosed in a quartz cuvette with 1 mm optical path and placed into discharge container to accept the UV irradiation generated by discharge plasma. Raman spectra of the sample with and without the UV irradiation were acquired and shown in Figure S4. It is clear from the figure that sole UV irradiation generated during plasma treatment cannot induce any detectible damage to GSH. However, its effect on radical intermediates cannot be excluded, but this cannot be detected by Raman spectroscopy in our experiment.

In the presence of oxygen, such as under normal physiological conditions, thiyl radicals react rapidly with oxygen to form sulfur peroxyl radicals ($GSOO^{\bullet}$) in competition with reaction (6)–(8), followed by chain reactions to form various other oxidizing radicals, such as $RSO_2^{\bullet}$, $RSO^{\bullet}$, $RSO_2OO^{\bullet}$, and so on (Scheme 1 in Supporting Information),[34,65,66] which may induce oxidative damage to biomolecules in cells.[67] It is therefore expected that severer GSH damage will occur under oxygen than under argon, as for the γ-irradiation of cysteine solution,[50] which is due to the participation of oxygen in reactions and longer chain reactions occurred. For this purpose, another set of experiments were carried out in which oxygen was imported into GSH solution before discharge for 10 min and used as the discharge atmosphere later. The rate constant k for GSH damage under this condition was determined by Raman spectroscopy as described above and its value was 0.13 min^{-1} (see Figure S5 in Supporting Information), higher than the value under argon atmosphere ($k = 0.11\ min^{-1}$). The data qualitatively confirmed that oxygen atmosphere can reliably induce severer GSH damage by discharge plasma treatment. The actual effect of atmosphere on the reaction rate is possibly more pronounced than we detected because oxygen is generated in solution by discharge plasma treatment.

4. Conclusion

With the help of Raman measurements, the GSH–GSSG system under discharge plasma was investigated. The content of GSH decreased exponentially with the discharge time, while in the meantime, the concentration of GSSG increased exponentially. The proportion of GSH converted to GSSG was approximately 30–40%, and 70–60% reduced GSH was converted to other products. Sulfhydryl groups were the main target attacked by the reactive species produced in solution during the discharge. This study shows that through Raman spectroscopy the GSH–GSSG conversion by discharge plasma can be evaluated quickly and accurately. The results shown in this paper may be helpful for understanding the effect of discharge plasma on the antioxidant system of biological organisms. As the concentration ratio of GSH to GSSG can be used as an index for oxidative stress under various conditions, this study may also open a new door to the quantitative investigation of the oxidasive stress effect on biological systems due to extrinsic oxidative agents such as discharge plasma.

Acknowledgements: This work was supported by the Natural Science Foundation of China (no. 10975152, no. 11175204), the Key Innovative Project of the Chinese Academy of Sciences (no. KJCX2-YW-N34-1), and the One-Hundred-Talent Program of the Chinese Academy of Sciences.

Received: March 29, 2012; Revised: August 18, 2012; Accepted: September 7, 2012; DOI: 10.1002/ppap.201200047

Keywords: free radicals; non-thermal plasma; optical spectroscopy; peptides

[1] T. Cserfalvi, P. Mezie, *J. Anal. At. Spectrom.* **1994**, *9*, 345.
[2] Y. Shimizu, K. Kawaguchi, T. Sasaki, N. Koshizaki, *Appl. Phys. Lett.* **2009**, *94*, 191504.
[3] C. Richmonds, R. M. Sankaran, *Appl. Phys. Lett.* **2008**, *93*, 131501.
[4] S. A. Meiss, M. Rohnke, L. Kienle, S. Zein El Abedin, F. Endres, J. Janek, *ChemPhysChem* **2007**, *8*, 50.
[5] W. F. L. M. Hoeben, E. M. van Veldhuizen, W. R. Rutgers, G. M. W. Kroesen, *J. Phys. D: Appl. Phys.* **1999**, *32*, L133.
[6] Z. G. Ke, Q. Huang, H. Zhang, Z. L. Yu, *Environ. Sci. Technol.* **2011**, *45*, 7841.
[7] J. Li, T. C. Wang, N. Lu, D. D. Zhang, Y. Wu, T. W. Wang, M. Sato, *Plasma Sources Sci. Technol.* **2011**, *20*, 034019.
[8] J. L. Brisset, B. Benstaali, D. Moussa, J. Fanmoe, E. Njoyim-Tamungang, *Plasma Sources Sci. Technol.* **2011**, *20*, 034021.
[9] D. D. Shao, Z. Q. Jiang, X. K. Wang, *Plasma Process. Polym.* **2010**, *7*, 552.
[10] D. D. Shao, J. Hu, X. K. Wang, *Plasma Process. Polym.* **2010**, *7*, 977.
[11] X. Ren, D. D. Shao, G. X. Zhao, G. D. Sheng, J. Hu, S. T. Yang, X. K. Wang, *Plasma Process. Polym.* **2011**, *8*, 589.
[12] X. Yan, Z. L. Xiong, F. Zou, S. S. Zhao, X. P. Lu, G. X. Yang, G. Y. He, K. Ostrikov, *Plasma Process. Polym.* **2012**, *9*, 59.
[13] Q. Xin, X. W. Zhang, L. C. Lei, *Plasma Chem. Plasma Process.* **2008**, *28*, 689.
[14] J. Ehlbeck, U. Schnabel, M. Polak, J. Winter, T. v. Woedtke, R. Brandenburg, T. V. D. Hagen, K.-D. Weltmann, *J. Phys. D: Appl. Phys.* **2011**, *44*, 013002.
[15] S. K. Kang, M. Y. Choi, I. I. G. Koo, P. Y. Kim, Y. Kim, G. J. Kim, A.-A. H. Mohamed, G. J. Collins, J. K. Lee, *Appl. Phys. Lett.* **2011**, *98*, 143702.
[16] N. Bai, P. Sun, H. X. Zhou, H. Y. Wu, R. X. Wang, F. X. Liu, W. D. Zhu, J. L. Lopez, J. Zhang, J. Fang, *Plasma Process. Polym.* **2011**, *8*, 424.
[17] M. A. Mottaleb, J. S. Yang, H. J. Kim, *Appl. Spectrosc. Rev.* **2002**, *37*, 247.
[18] S. M. Thagard, K. Takashima, A. Mizuno, *Plasma Chem. Plasma Process.* **2009**, *29*, 455.
[19] P. Mezei, T. Cserfalvi, *Appl. Spectrosc. Rev.* **2007**, *42*, 573.
[20] M. Moisan, J. Barbeau, M. C. Crevier, J. Pelletier, N. Philip, B. Saoudi, *Pure Appl. Chem.* **2002**, *74*, 349.
[21] X. Yan, F. Zou, X. P. Lu, G. Y. He, M. J. Shi, Q. Xiong, X. Gao, Z. L. Xiong, Y. Li, F. Y. Ma, M. Yu, C. D. Wang, Y. S. Wang, G. X. Yang, *Appl. Phys. Lett.* **2009**, *95*, 083702.
[22] G. Li, H. P. Li, L. Y. Wang, S. Wang, H. X. Zhao, W. T. Sun, X. H. Xing, C. Y. Bao, *Appl. Phys. Lett.* **2008**, *92*, 221504.
[23] X. T. Deng, J. J. Shi, M. G. Kong, *J. Appl. Phys.* **2007**, *101*, 074701.
[24] X. T. Deng, J. J. Shi, H. L. Chen, M. G. Kong, *Appl. Phys. Lett.* **2007**, *90*, 013903.
[25] J. Julák, O. Janoušková, V. Scholtz, K. Holada, *Plasma Process. Polym.* **2011**, *8*, 316.
[26] H. P. Li, L. Y. Wang, G. Li, L. H. Jin, P. S. Le, H. X. Zhao, X. H. Xing, C. Y. Bao, *Plasma Process. Polym.* **2011**, *8*, 224.
[27] H. Yasuda, M. Hashimoto, M. M. Rahman, K. Takashima, A. Mizuno, *Plasma Process. Polym.* **2008**, *5*, 615.
[28] E. Takai, K. Kitano, J. Kuwabara, K. Shiraki, *Plasma Process. Polym.* **2012**, *9*, 77.
[29] Z. G. Ke, Q. Huang, X. Su, J. Jiang, X. Q. Wang, Z. L. Yu, *Nucl. Instrum. Methods Phys. Res. Section B* **2010**, *268*, 1618.
[30] Z. G. Ke, Q. Huang, B. G. Dang, Y. L. Lu, H. Yuan, S. Q. Zhang, *Nucl. Instrum. Methods Phys. Res. Section B* **2010**, *268*, 2729.
[31] X. Su, Q. Huang, B. R. Dang, X. Q. Wang, Z. L. Yu, *Radiat. Phys. Chem.* **2011**, *80*, 1343.
[32] H. J. Forman, H. Q. Zhang, A. Rinna, *Mol. Aspects Med.* **2009**, *30*, 1.
[33] A. Meister, *J. Biol. Chem.* **1988**, *263*, 17205.
[34] M. Tamba, A. Torreggiani, *Res. Chem. Intermed.* **2002**, *28*, 57.
[35] O. W. Griffith, *Free Radic. Biol. Med.* **1999**, *27*, 922.
[36] P. Monostori, G. Wittmann, E. Karg, S. Túri, *J. Chromatogr. B* **2009**, *877*, 3331.
[37] J. Filik, N. Stone, *Analyst* **2007**, *132*, 544.
[38] D. M. Zhang, D. P. Jiang, M. Yanney, S. Zou, A. Sygula, *Anal. Biochem.* **2009**, *391*, 121.
[39] D. M. Zhang, M. F. Mrozek, Y. Xie, D. Ben-Amotz, *Appl. Spectrosc.* **2004**, *58*, 929.
[40] D. M. Zhang, Y. Xie, M. F. Mrozek, C. Ortiz, V. Jo Davisson, D. Ben-Amotz, *Anal. Chem.* **2003**, *75*, 5703.
[41] Y. Xie, D. M. Zhang, G. K. Jarori, V. Jo Davisson, D. Ben-Amotz, *Anal. Biochem.* **2004**, *332*, 116.
[42] C. Ortiz, D. M. Zhang, Y. Xie, V. Jo Davisson, D. Ben-Amotz, *Anal. Biochem.* **2004**, *332*, 245.
[43] R. A. Halvorson, P. J. Vikesland, *Environ. Sci. Technol.* **2011**, *45*, 5644.
[44] R. A. Halvorson, W. N. Leng, P. J. Vikesland, *Anal. Chem.* **2011**, *83*, 9273.
[45] R. D. Deegan, O. Bakajin, T. F. Dupont, G. Huber, S. R. Nagel, T. A. Witten, *Nature* **1997**, *389*, 827.
[46] W. Ando, K. Sugimoto, S. Oae, *Bull. Chem. Soc. Jpn.* **1963**, *36*, 893.
[47] N. T. Yu, D. C. DeNagel, P. L. Pruett, J. F. R. Kuck, Jr., *Proc. Natl. Acad. Sci. USA* **1985**, *82*, 7965.
[48] M. A. Rosei, *Cell. Mol. Life Sci.* **1979**, *36*, 955.
[49] W. M. Garrison, *Chem. Rev.* **1987**, *87*, 381.
[50] J. E. Packer, R. V. Winchest, *Can. J. Chem.* **1970**, *48*, 417.
[51] A. P. Senft, T. P. Dalton, H. G. Shertzer, *Anal. Biochem.* **2000**, *280*, 80.
[52] G. Compagnini, A. Licciardello, L. Romano, O. Puglisi, *Nucl. Instrum. Methods Phys. Res. Section B* **1996**, *116*, 242.
[53] M. Z. Hoffman, E. Hayon, *J. Phys. Chem.* **1973**, *77*, 990.
[54] M. Lal, *Can. J. Chem.* **1976**, *54*, 1092.
[55] S. Budavari, Ed., "*The Merck Index*," Merck and Co. Publishers, New Jersey **1989**.
[56] T. E. Eriksen, G. Fransson, *J. Chem. Soc. Perkin Trans. 2* **1988**, 1117.
[57] L. Grierson, K. Hildebrand, E. Bothe, *Int. J. Radiat. Biol.* **1992**, *62*, 265.
[58] K. P. Arjunan, A. M. Clyne, *Plasma Process. Polym.* **2011**, *8*, 1154.
[59] S. Kanazawa, H. Kawano, S. Watanabe, T. Furuki, S. Akamine, R. Ichiki, T. Ohkubo, M. Kocik, J. Mizeraczyk, *Plasma Sources Sci. Technol.* **2011**, *20*, 034010.
[60] B. R. Locke, K. Y. Shih, *Plasma Sources Sci. Technol.* **2011**, *20*, 034006.
[61] I. Safarik, O. Straus, *Res. Chem. Intermed.* **1985**, *6*, 143.
[62] F. E. Littman, E. M. Carr, A. P. Brody, *Radiat. Res.* **1957**, *7*, 107.
[63] P. Markakis, A. L. Tappel, *J. Am. Chem. Soc.* **1960**, *82*, 1613.
[64] G. Navon, G. Stein, *Israel J. Chem.* **1964**, *2*, 151.
[65] M. Tamba, G. Simone, M. Quintiliani, *Int. J. Radiat. Biol.* **1986**, *50*, 595.
[66] Z. Abedinzadeh, *Can. J. Physiol. Pharmacol.* **2001**, *79*, 166.
[67] M. D. Sevilla, D. Becker, M. Yan, *Int. J. Radiat. Biol.* **1990**, *57*, 65.

DOI: 10.1002/ppap.201200047